

Synthesis and characterization of polysilicic acid nanoparticles/waterborne polyurethane nanocomposite

HSU-CHIANG KUAN, HSUN-YU SU, CHEN-CHI M. MA*

Department of Chemical Engineering, National Tsing Hua University, HsinChu, Taiwan, 300
E-mail: ccma@che.nthu.edu.tw

Published online: 8 September 2005

A novel nanocomposite that consists of polysilicic acid nanoparticles (PSA)/waterborne polyurethane (WPU) was prepared. The nano-size distribution of PSA particles were measured using the dynamic light scattering method. Nanocomposites were monitored and characterized by Fourier-Transform Infrared spectrophotometer (FT-IR). Si-mapping was used to elucidate the dispersion of silica in the nanocomposite. Morphological investigations revealed that PSA nanoparticles were well dispersed in waterborne polyurethane matrix on the nano-scale (100 nm). Thermal characteristics indicated that adding PSA increased the thermal degradation temperature by 43°C when the content of polysilicic acid nanoparticles was 5 wt%. Mechanical property tests demonstrated that adding polysilicic acid nanoparticles improved the tensile properties (by more than 100%), and reduced the wear index. Oxygen permeability tests showed that introducing the PSA nanoparticles increased the oxygen permeability of the nanocomposite.

© 2005 Springer Science + Business Media, Inc.

1. Introduction

In the past decade, the synthesis and characterization of inorganic-organic hybrid materials by the sol-gel process have received great attention [1–3]. For example, flexible polymers with high modulus, along with the high thermal stability and good optical properties of inorganic glasses can be prepared. The properties of the inorganic-organic hybrid materials are dependent on the nature and relative content of the constitutive inorganic and organic components [4–7]. The basic sol-gel process involves the hydrolysis and polycondensation reactions of metal or silicon alkoxide, e.g. $\text{Si}(\text{OEt})_4$ or $\text{Si}(\text{OMe})_4$, which are governed by the value of pH, solvent, catalyst and temperature [8]. The drawbacks of traditional sol-gel process are the tedious preparation procedure and the difficulty to control the reaction.

Polyurethane (PU) is globally used on a large scale for adhesive, coating, and cast applications due to its high toughness, high impact strength, and so on. The phase separation between inorganic and organic components may take place and will deteriorate the properties of the materials [1]. Water dispersions, lattices or emulsions of polyurethane elastomers or coating permit the application of polyurethanes from an aqueous medium. For waterborne polyurethane (WPU) systems, only water was evaporated during the drying process, thus rendering these systems safe with regard to

the environment. They are non-toxic, non-flammable and do not generate polluted air or wastewater [10–13].

With the aim of exploring the so-called “high-performance” materials, a combination of organic polymers with inorganic materials has been examined. Addition of a filler of ultrafine particle such as silica gel, polysilicic acid nanoparticles, calcium carbonate, or carbon black to organic polymer has been utilized to prepare composite materials of high strength [14–20].

Composites containing polysilicic acid nanoparticles (PSA) is one of the most interesting research topics in the recent years [21–23]. The polysilicic acid nanoparticles, which contain many silanol groups on the surface of the particle, which could be directly, incorporated with the SiOEt groups in the waterborne polyurethane (WPU). When the solvent and water were removed, the nanocomposites were obtained.

This study presents the novel synthesis approach of nanocomposites from waterborne polyurethane and polysilicic acid nanoparticles. This modified sol-gel process overcame the drawbacks of the traditional sol-gel process, and eliminated the need for a tedious manufacturing procedure. Several characterizations measurements of nanocomposite were also conducted in this study. The thermal mechanical properties and oxygen permeability of hybrid materials with various ratios of WPU/PSA were studied.

*Author to whom all correspondence should be addressed.

2. Experimental

2.1. Materials

The 3-isocyanatomethyl-3,5,5-trimethyl-cyclohexylisocyanate (IPDI) was purchased from the TCI Co., Tokyo, Japan. Neopentylglycol (NPG) and Polycaprolactone (PCL) with molecular weight 1250 were obtained from Solvay Interlox Company, Cheshire, U.K. The catalyst, stannous 2-ethylhexanoate, is purchased from Sigma-Aldrich Co., USA. Emulsifier used in this study is sulfonate tertiary amine (DS-200, MW ~ 250), which is received from HOPAX company, Taiwan. Coupling agent used is 3-aminopropyl-triethoxysilane (APTS) (Fluka, Chemicals, Milwaukee, WI, USA); Sodium metasilicate nonahydrate was received from Acros Organics, Geelwest, Belgium.

2.2. Synthesis of polysilicic acid nanoparticles/waterborne polyurethane nanocomposite

2.2.1. Preparation of polysilicic acid nanoparticles (PSA)

30 g sodium metasilicate ($\text{Na}_2\text{SiO}_3 \cdot 9\text{H}_2\text{O}$) was dissolved in 10^{-4} m^3 water and then added the solution into $2.5 \text{ N } 10^{-4} \text{ m}^3$ hydrochloric acid solution with stirring at 0°C in 10 min. Then 10^{-4} m^3 THF and 60 g NaCl were added into the solution subsequently. After stirring vigorously for 15 min, the reaction mixture was allowed to stand for 10 min. The organic layer (THF layer) was separated and dried with 30 g of anhydrous sodium sulfate. The size of the PSA particles in THF solution was investigated by dynamic light scattering (DLS) measurement. The synthesis procedures were shown in [Scheme 1](#).

2.2.2. Preparation of WPU/PSA hybrid materials

The prepolymer was prepared by reacting 0.025 mol PCL, 0.11 mol IPDI and $2 \times 10^{-7} \text{ m}^3$ stannous 2-ethylhexanoate with acetone at 70°C for 8 h, then 0.0125 mol of DS-200 (contain sulfonic acid group) was (dissolved in THF solution) added and stirred at 70°C for 5 h 0.0375 mol NPG was added into the polymer solution at 70°C for 3 h. The solution of 0.025 mol coupling agent in $5 \times 10^{-5} \text{ m}^3$ DI water was dropped into the polymer solution by micro-tube pump. Then the preparation of WPU was completed.

PSA-THF solution was added into the WPU solution according to the different contents of 0, 5, 10, 15, 20 wt% of PSA. The mixture was stirred at room temperature for 1 h. Films of hybrid materials with uniform thickness were then obtained by removing THF and excess H_2O in vacuum at 100°C after the mixing. The synthesis procedures were shown in [Scheme 2](#).

2.3. Characterization and property measurements

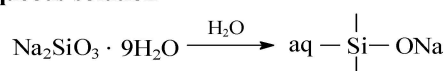
2.3.1. Dynamic light scattering (DLS) measurement

The DLS measurement for particle size distribution of PSA was performed with a Malvern series 4700 apparatus (Malvern Instrument, Worcestershire, UK). A 2W argon-ion laser operating at a power of 500 mW with a wavelength of 514.5 nm was used as the light source, which was focused on the sample cell within the temperature $25.0 \pm 0.1^\circ\text{C}$, and with the scattering angle at 90° .

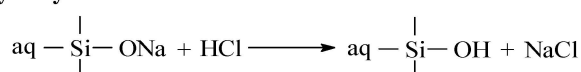
2.3.2. Fourier transfer infrared spectroscopy (FT-IR)

FT-IR spectra of polysilicic acid nanoparticles/waterborne polyurethane nanocomposite were

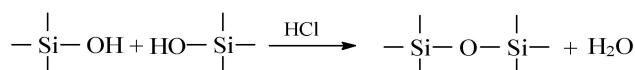
Aqueous solution



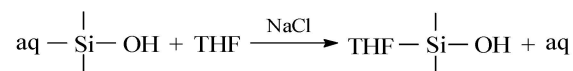
Hydrolysis



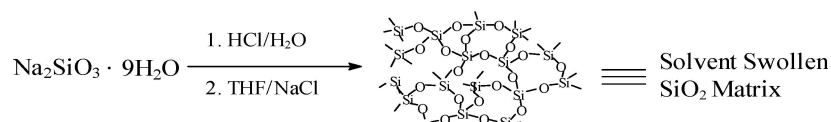
Condensation



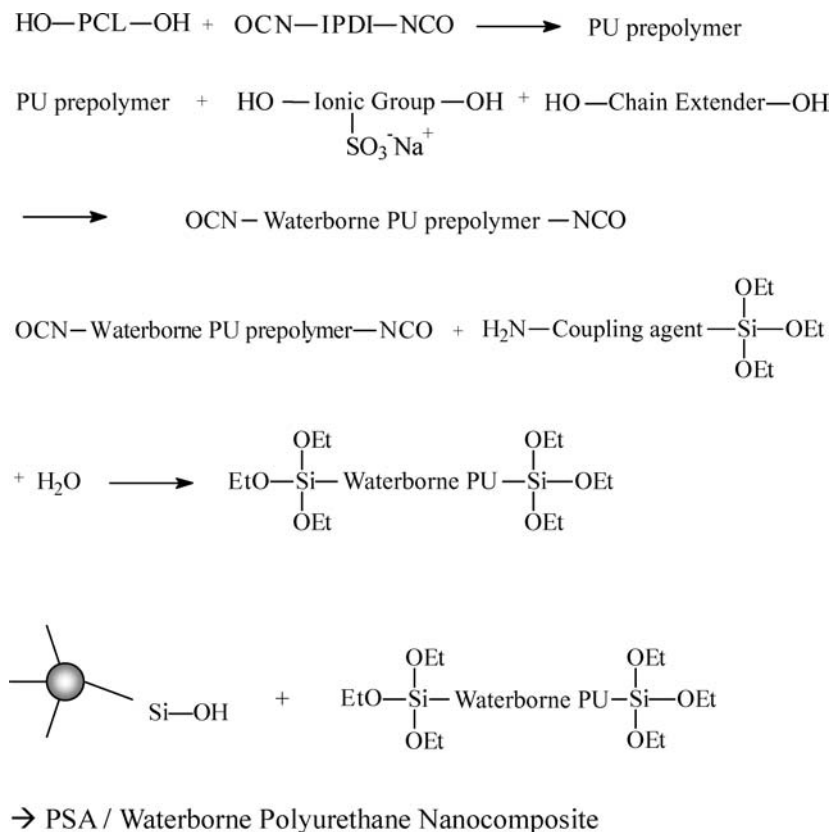
Extraction



Net Reaction



Scheme 1 Procedures for preparing polysilicic acid nanoparticles.



Scheme 2 The synthesis mechanism of polysilicic acid nanoparticles/waterborne polyurethane nanocomposites.

recorded between 400–4000 cm^{-1} on a Nicolet Avatar 320 FT-IR spectrometer, Nicolet Instrument Corporation, Madison, WI, U.S.A. The polysilicic acid nanoparticles/waterborne polyurethane nanocomposite sample was coated on a KBr plate. A minimum of 32 scans was signal averaged with a resolution of 2 cm^{-1} within the 400–4000 cm^{-1} range. The characteristic absorption peaks of functional group were detected and monitored during the synthesis reaction such as N–H stretching at 3500 cm^{-1} , O–H stretching at 3300 cm^{-1} , NCO stretching at 2270 cm^{-1} , C=O stretching of urethane at 1740 cm^{-1} , C=O stretching of urea at 1660 cm^{-1} and Si–O asymmetric stretching at 1150 cm^{-1} .

2.3.3. Scanning electronic microscopy (SEM)

Surface morphology of polysilicic acid nanoparticles/waterborne polyurethane nanocomposite were investigated by Scanning Electron Microscope (HITACHI-S4700, S570, Tokyo, Japan). The fracture surfaces were sputter coated with gold prior to scanning. The distributions of Si atoms in the hybrid creamers were obtained from SEM EDX mapping. The white points in the figures denote the Si atoms.

2.3.4. Tensile properties

Polysilicic acid nanoparticles/waterborne polyurethane film were cut into dumb-bells shape according to the ASTM D683 testing method by Instron testing machine (type: Mini 44). The crosshead speed was 2 mm/min.

The dimensions of samples were 6.0 × 5.0 × 1.4 mm (length × width × thickness). Six specimens were tested in each case. All tests were performed at ambient temperature of 25 ± 2°C.

2.3.5. Wear properties

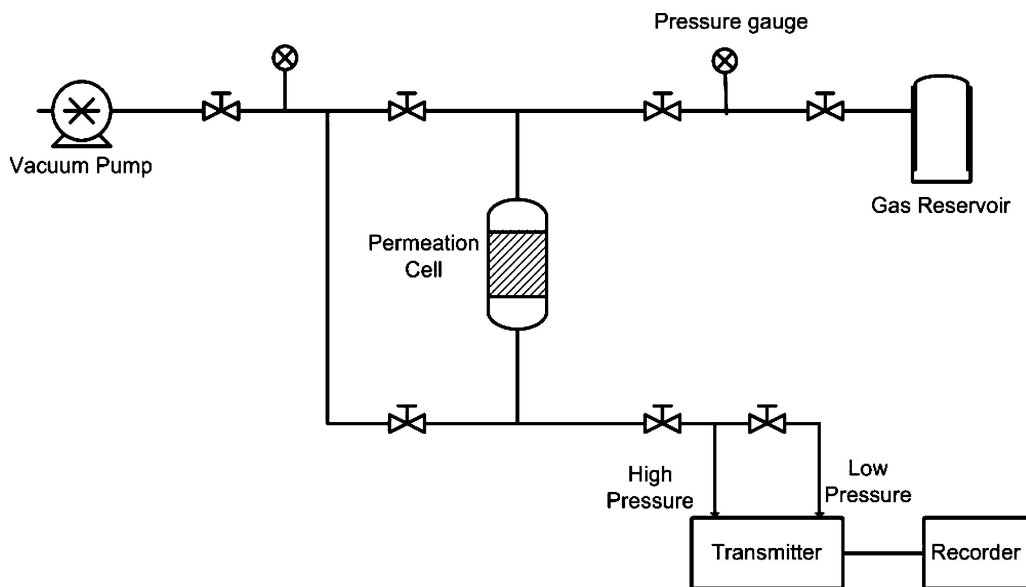
A 10 × 10 cm film was prepared and then fixed it on wearing machine (type: PT-3050 Taber, Perfect International Instrument., Taiwan) with 1 kg load. The weight loss was measured after 500, 1000, 1500, 2000 and 3000 wearing cycles by ASTM D4060-90 method. The wear index I was calculated as: $I = ((W_1 - W_2)/C) \times 1000$, where W_1 is the original weight of sample, W_2 is the weight after wearing, and C is the wearing cycles.

2.3.6. Differential scanning calorimeter (DSC) analysis

Samples were carried out for differential scanning calorimeter (DSC) analysis under a N_2 atmosphere with a TA Instruments DSC 10 (U.S.A.). Samples were first placed in a vacuum oven at 100°C for 24 h before being sealed in an aluminum sample cell then held at 100°C for 10 min and was quickly put into liquid nitrogen until the temperature reached at –100°C to obtain amorphous samples. These amorphous samples were then heated again to 100°C at a heating rate of 10°C/min.

2.3.7. Gas permeability

Pure oxygen permeability of nanocomposite film (80–100 μm) was collected by apparatus shown in



Scheme 3 The apparatus for gas permeability measurement.

Scheme 3. The permeability coefficient, diffusivity coefficient and solubility coefficient were calculated by the following equations:

(a) Permeability coefficient, P , was determined by Equation 1 at the steady state.

$$P = \frac{273 \times V \times L \times \frac{dp}{dt}}{760 \times T \times A \times (P_u - P_d)} \quad (1)$$

where $\frac{dp}{dt}$ is the derivative of P_d versus t , L is film thickness, V is the volume of permeation cell, T is the temperature, A is the cross section area of nanocomposite film, P_u and P_d is the input and output pressure of film (but $P_u \gg P_d$).

(b) Diffusivity coefficient, D , was determined by time-lag method, as Equation 2:

$$D = \frac{L^2}{6\Theta} \quad (2)$$

where Θ is the time value of straight line crossing the time-axis in the figure of P_d versus t .

(c) Solubility coefficient, S , was determined by Equation 3:

$$P = D \times S \quad (3)$$

3. Results and discussion

3.1. Particle size of PSA

The particle size of PSA prepared by hydrolysis and condensation of sodium metasilicate in 2.5 N HCl solution was measured by DLS. Fig. 1 indicates that the particle size of PSA range from 3 to 25 nm, and the average size is 9 nm in THF solution in the steady state. PSA particles can be effectively dispersed in THF solution on the nano scale, so PSA can be dispersed in waterborne polyurethane prepolymer to form the nanocomposite using conventional stirring machine.

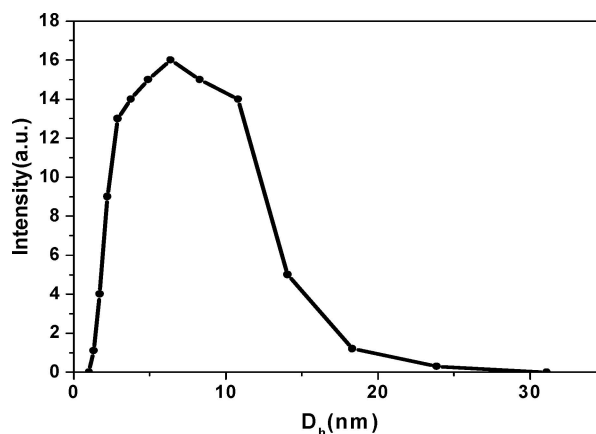


Figure 1 The particle size distribution of PSA in THF solution at steady state.

3.2. Characterization of waterborne polyurethane

The structures of the polysilicic acid nanoparticle/waterborne polyurethane nanocomposite coatings were analyzed by FT-IR, as depicted in Fig. 2. Fig. 2a reveals that the $-\text{OH}$ group characteristic absorption peak was broad at 3200 cm^{-1} . It indicated that the hydroxyl group was attached to the surface of PSA nanoparticles. Fig. 2b indicates that the WPU reacted with coupling agent, because $\text{C}=\text{O}$ stretching associated with urea appeared at 1650 cm^{-1} . It also demonstrates an asymmetric stretching of $\text{S}=\text{O}$ at 1150 cm^{-1} . The $\text{S}=\text{O}$ absorption peak revealed that sulfonic acid emulsifying agent was grafted to the polymer chain. When the reaction was completed, the $\text{N}=\text{C}=\text{O}$ stretching group of IPDI at 2270 cm^{-1} disappeared completely. The $\text{C}=\text{O}$ stretching of urethane at 1735 cm^{-1} appeared and became stronger in the second step. The asymmetric stretching peak of $\text{Si}-\text{O}-\text{Si}$ bonding at 1100 cm^{-1} was also clear.

3.3. Morphological characteristics

The morphology of the fractured surfaces was observed using SEM. The mapping technique was employed

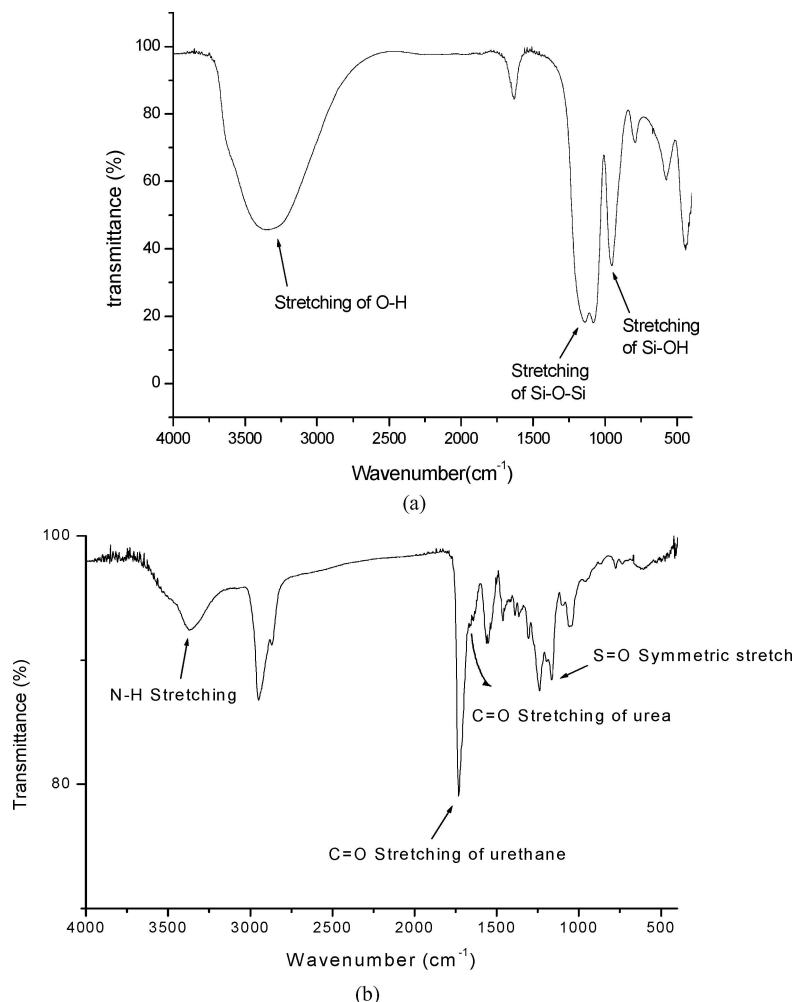


Figure 2 (a) FT-IR spectra of PSA nanoparticle and (b) FT-IR spectrum of polysilicic acid nanoparticles/waterborne polyurethane nanocomposites for functional group identification.

to elucidate the distribution of PSA nanoparticles in a hybrid matrix. Figs 3 and 4 present the SEM microphotographs and the EDX Si-mapping of polysilicic acid nanoparticles/waterborne polyurethane nanocomposites. In Figs 2 and 4, the white dots represent the PSA nanoparticles. Fig. 3 reveals that the particles with 15 wt% PSA content in the polymer matrix were effectively dispersed, and the particle size was approximately 50 nm or smaller (since the limitation of SEM, the particle size of PSA that can be observed and recognized is around 50 nm). Fig. 4 illustrates the aggregation of PSA nanoparticles when the content exceeded 20 wt%.

3.4. Thermal degradation characteristics

Fig. 5 shows that adding more PSA nanoparticles to the polymer matrix increases the thermal degradation temperature of hybrid materials. For instance, the thermal degradation temperature associated with 10% weight loss was 269.2°C for pristine waterborne polyurethane, 312.6°C for the nanocomposites with 5 wt% PSA content and 332.4°C for the nanocomposites with 20 wt% PSA. PSA nanoparticles are inorganic material that exhibits heat-resistance, so the presence of PSA nanoparticles can retard thermal degradation or delay the onset of the thermal degradation of the polystyrene. The char

yield of nanocomposites increased with PSA nanoparticles content. PSA nanoparticles are more thermally stable than waterborne polyurethane. The effective dispersion of PSA nanoparticles in the polyurethane matrix can enhance the thermal stability of nanoparticles, increasing the thermal degradation temperature of the organic-inorganic hybrid.

3.5. Mechanical properties

3.5.1. Tensile properties

Table I summarizes the tensile properties of polysilicic acid nanoparticles/waterborne polyurethane nanocomposite. Adding polysilicic acid nanoparticles to waterborne polyurethane increase the initial tensile modulus of the composites. The tensile modulus of the

TABLE I Tensile property of polysilicic acid nanoparticles/waterborne polyurethane nanocomposites (soft segment molecular weight 1250) nanocomposite with different PSA contents

Silica contents (wt%)	Young's modulus (MPa)	Max stress (MPa)	Elongation at break (%)
0	20.2	0.97	210
5	29.5	1.53	57.2
10	32.1	2.55	58.7
15	35.9	4.59	54.6
20	40.8	4.02	44.7

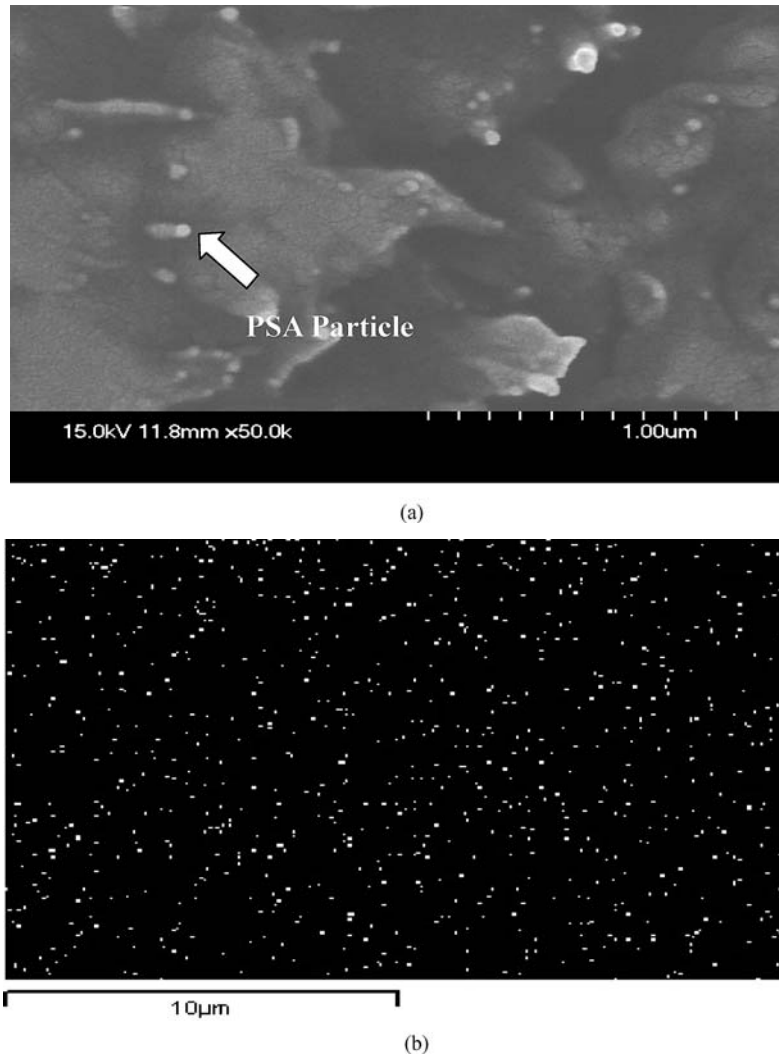


Figure 3 (a) SEM of WPU/15% PSA nanoparticles and (b) Si mapping of WPU/15%PSA nanoparticles.

polysilicic acid nanoparticles/waterborne polyurethane nanocomposite with 20 wt% silica increased from 20.2 to 40.8 MPa (101.9%). The polysilicic acid nanoparticles play an important role in strengthening the composites by effectively transferring the stress between the silica and the polyurethane matrix.

3.5.2. Wear resistance

Fig. 6a and b indicate that the wear index declined as the particles content increased (below 15 wt%) over 500 and 1000 wear cycles. The wear index was proportional to the reciprocal of the wear-resistance. SEM revealed that the particles were well dispersed in the polymer matrix, suggesting that the nanocomposites exhibit good miscibility between organic and inorganic phases, so the wear resistance was enhanced by wear-endurable PSA nanoparticle. The wear-resistance of the nanocomposites was greatest at 15 wt% PSA nanoparticle content.

3.6. Oxygen permeability

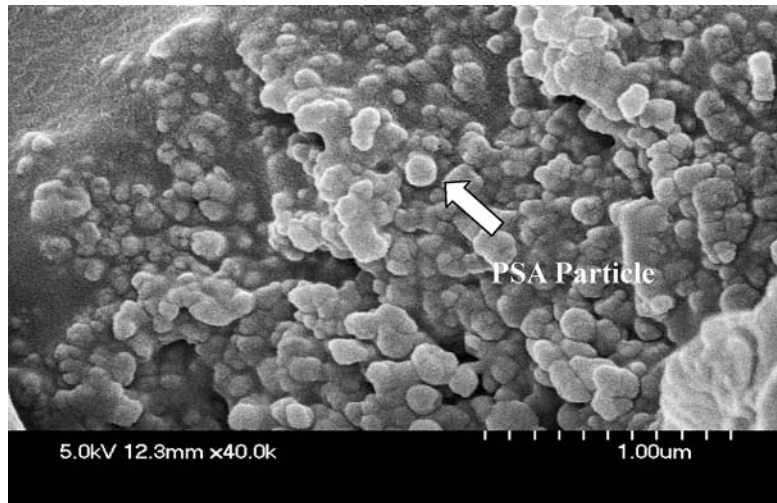
The oxygen permeability of nanocomposite doubled increased from $4.56 \times 10^{-11}(\text{cc} \cdot (\text{STP}) \cdot \text{cm}) / (\text{cm}^2 \cdot \text{sec} \cdot \text{cmHg})$ to $9.24 \times 10^{-11}(\text{cc} \cdot (\text{STP}) \cdot \text{cm}) / (\text{cm}^2 \cdot \text{sec} \cdot \text{cmHg})$ when the PSA content was 20 wt%, as indicated in Table II. Table II also reveals that the diffusivity coef-

TABLE II Oxygen permeation properties of WPU nanocomposites with different PSA contents

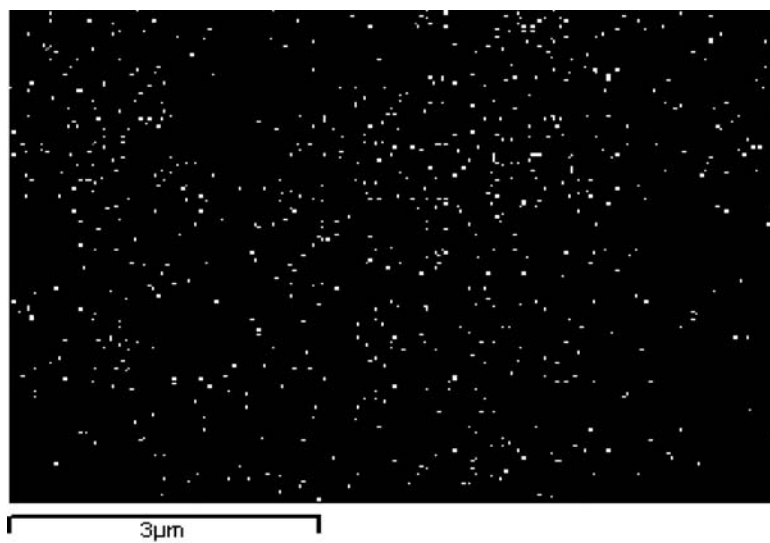
PSA contents (wt%)	$P (\times 10^{11})$	$D (\times 10^8)$	$S (\times 10^3)$
0	4.56	1.21	3.76
5	7.55	16.8	0.45
10	8.17	13.4	0.61
15	8.71	22.3	0.39
20	9.24	20.3	0.46

ficient increased and the solubility coefficient fell as the PSA content increased. The PSA particles increased the free volume of polymer chain folding then increasing the number of void of nanocomposite, that reducing the mean free path of oxygen molecules, increasing the oxygen diffusivity. However, oxygen is a non-polar gas, so adding polar PSA nanoparticle to nanocomposite reduces the solubility of oxygen. These two effects compete; the oxygen permeability of nanocomposite was increased by adding PSA nanoparticles after all.

To prove the free volume change, a dynamic scanning calorimeter (DSC) was used to observe the T_g of nanocomposite. The results show that the T_g s of waterborne polyurethane, PSA/WPU nanocomposites with 5 wt%, 10 wt%, 15 wt%, 20 wt% PSA contents are -44.5°C , -33.5°C , -27.2°C , -24.1°C and -19.2°C ,



(a)



(b)

Figure 4 (a) SEM of WPU/20% PSA nanoparticles and (b) Si mapping of WPU/20% PSA nanoparticles.

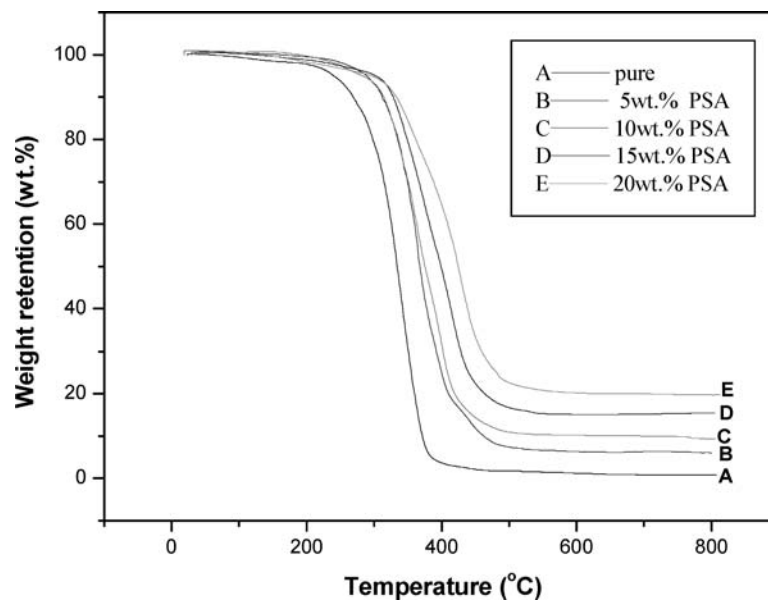
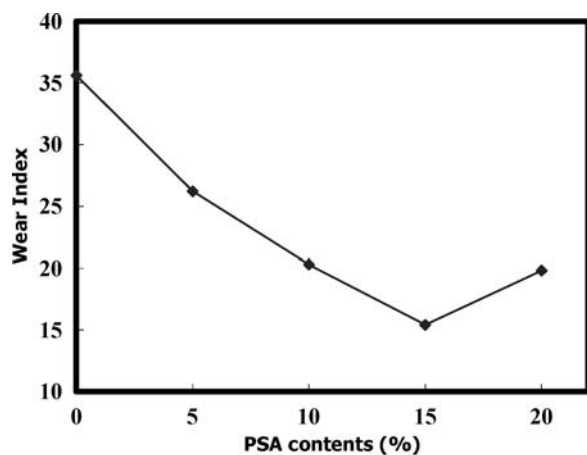
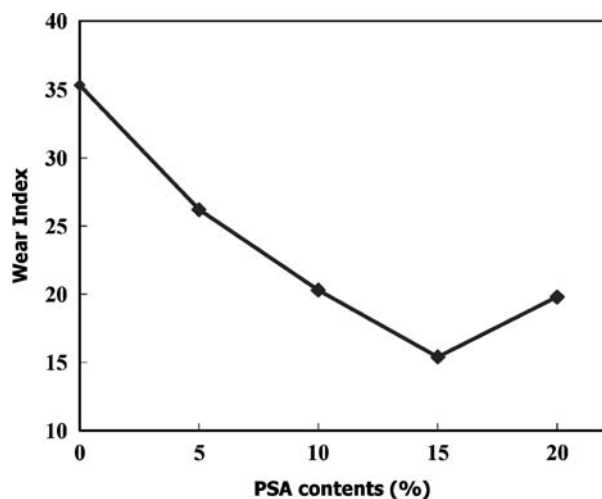


Figure 5 TGA results of polysilicic acid nanoparticles/waterborne polyurethane nanocomposites with different polysilicic acid nanoparticle contents.



(a)



(b)

Figure 6 (a) Wear index of polysilicic acid nanoparticles/waterborne polyurethane nanocomposites under 500 wear cycles and (b) Wear index of polysilicic acid nanoparticles/waterborne polyurethane nanocomposites under 1000 wear cycles.

respectively. From the results of T_g measurements, it may be concluded that the free volume of nanocomposite increase as the increase of PSA content.

4. Conclusions

Polysilicic acid nanoparticles/waterborne polyurethane nanocomposites were successfully synthesized. This modified sol-gel process overcame the drawbacks of the traditional sol-gel process, and eliminated the need for a tedious manufacturing procedure. FT-IR was used to characterize the nanocomposite. SEM microphotographs and Si-mapping of polysilicic acid nanoparticles/waterborne polyurethane nanocomposite indicated that polysilicic acid nanoparticles were well dispersed in waterborne polyurethane. TEM microphotographs revealed that the size of polysilicic acid nanoparticles that remained in waterborne polyurethane nanocomposite was around 100 nm, indicating nano-dispersion in the nanocomposites. The thermal properties of the nanocomposite, measured by TGA, demonstrated that adding polysilicic acid nanoparticles increased the temperature of thermal degradation by 63°C when the PSA nanoparticles were 20 wt%. Mechanical property tests showed that adding polysilicic acid nanoparticles improved the tensile properties (The tensile modulus in-

creased by 101.9% when the polysilicic acid nanoparticles content was 20 wt%). The wear properties of polysilicic acid nanoparticles/waterborne polyurethane nanocomposite were considerably improved. Introducing the PSA nanoparticles increased the oxygen permeability of the nanocomposite.

Acknowledgement

The authors would like to acknowledge the National Science Council, Taiwan, Republic of China, for the financially supporting this research under the contract No.: NSC 92-2216-E-007-024.

References

1. G. L. WIKES, H. H. HUANG and R. H. GLASER, in "Silicon-Based Polymer Science, Advances in Chemistry Series 224" (American Chemical Society, Washington, DC, 1990) p. 207.
2. G. PHILIP and H. SCHMIDT, *J. Non-Cryst. Solids* **63** (1984) 283.
3. J. E. MARK, C. JIANG and M. Y. TANG, *Macromolecules* **17** (1984) 2616.
4. J. D. MACKENZIE and Y. J. CHUNG, *J. Non-Cryst. Solids* **147** (1992) 271.
5. Y. G. HSU and F. J. LIN, *J. Appl. Polym. Sci.* **75** (2000) 275.
6. A. B. NRENNAN and G. L. WIKES, *Polymer* **332** (1991) 733.
7. D. TAN, P. DUBOIS and R. JEROME, *J. Polym. Sci. Polym. Chem.* **35** (1997) 2295.
8. C. J. BRINKER and G. W. SCHERER, in "Sol-Gel Science, the Physics and Chemistry of Sol-Gel Processing" (Academic Press, San Diego, 1990).
9. M. J. DVORCHAK, *J. Coat. Technol.* **69** (1997) 886.
10. V. DUECOFFRE, W. DIENER, C. FLOSBACH and W. SCHUBERT, *Prog. Org. Coat.* **34** (1998) 200.
11. C. H. YANG, H. J. YANG, T. C. WEN, M. S. WU and J. S. CHANG, *Polymer* **40** (1999) 871.
12. J. HUYBRECHTS, P. BRUYLANTS, A. VAES and A. DEMARRE, *Prog. Org. Coat.* **38** (2000) 67.
13. S. G. JOSE, F. G. TERESA and P. M. M. JOSE MIGUEL, *J. Adhes. Sci. Technol.* **15** (2001) 187.
14. A. M. TORRO-PALAU, J. C. FERNANDEZ-GARCIA and A. CESAR ORGILES-BARCELO, *Macromol. Symp.* **169** (2001) 191.
15. H. GODA and C. W. FRANK, *Chem. Mater.* **13** (2001) 2783.
16. A. M. TORRO-PALAU, J. C. FERNANDEZ-GARCIA, A. CESAR ORGILES-BARCELO and J. M. MARTIN-MARTINEZ, *Int. J. Adhes. Adhes* **21** (2001) 1.
17. R. C. R. NUNES, R. A. PEREIRA, J. L. C. FONSECA and M. R. PEREIRA, *Polym. Test.* **20** (2001) 707.
18. T. J. YIM, S. Y. KIM and K. P. YOO, *Kor. J. Chem. Eng.* **19** (2002) 159.
19. N. H. PARK, J. W. LEE and K. D. SUH, *J. Appl. Polym. Sci.* **84** (2002) 2327.
20. I. S. OH, N. H. PARK and K. D. SUH, *J. Appl. Polym. Sci.* **75** (2000) 968.
21. J. HABSUDA, G. P. SIMON, Y. B. CHENG, D. G. HEWITT, H. TOH and D. R. DIGGINS, *J. Polym. Sci. Pol. Chem.* **39** (2001) 1342.
22. C. S. WU and H. T. LIAO, *J. Polym. Sci. Pol. Phys.* **41** (2003) 351.
23. Y. YANG, Y. F. LU, M. C. LU, J. HUANG, R. HADDAD, G. XOMERITAKIS, N. LIU, A. P. MALANOSKI, D. STUMAYR, H. FAN, D. Y. SASAKI, R. A. ASSINK, J. A. SHELNUTT, V. S. FRANK, G. P. LOPEZ, A. R. BURNS and C. J. BRINKER, *J. Am. Chem. Soc.* **125** (2003) 1269.

Received 27 October 2004
and accepted 1 April 2005